Experimental Mechanics (2014) 54:393–403
DOI 10.1007/s11340-013-9813-7

Correction of Gauge Factor for Strain Gauges Used in Polymer Composite Testing

S. Zike · L.P. Mikkelsen

Received: 10 December 2012 / Accepted: 23 September 2013 / Published online: 9 October 2013

Abstract Strain gauges are used together with the corresponding gauge factor to relate the relative electrical resistance change of the strain gauge with the strain of the underlying material. The gauge factor is found from a calibration on a stiff material - steel. Nevertheless, the gauge factor depends on the stiffness of the calibration material and ideally the calibration should be done on a similar material as tested. In practice, the gauge factor found by the strain gauge manufacturer is often used. The paper documents that even for moderately stiff materials such as glass-fibre composites a significant error is found on the strain measurements obtained by the strain gauges. This is documented both experimentally and numerically. A stiffness, also test sample and strain gauge geometry dependent correction coefficient of the gauge factor is proposed. A correction coefficient covers material stiffnesses ranging from 1 GPa to 200 GPa.

Keywords Strain gauge · Strain measurements · Polymer material testing · Composites · Material characterization

S. Zike (✉) · L.P. Mikkelsen
Composites and Materials Mechanics Section, Department of Wind Energy, Technical University of Denmark, Risø Campus, 4000 Roskilde, Denmark
e-mail: zike@dtu.dk

L.P. Mikkelsen
e-mail: lapm@dtu.dk

Notations

A	parameter used for correction coefficient determination for the global reinforcement effect;
B	width;
C	correction coefficient;
C_0	permanent correction coefficient (depends on the strain gauge length);
E	Young's modulus;
E^*_{sg}	reduced Young's modulus of the strain gauge, which depends on the strain gauge stiffness and geometrical dimensions [10];
GF_{act}	actual gauge factor;
GF_{cal}	gauge factor provided by manufacturer (determined on a stiff calibration specimen);
L	length;
t	thickness;
t_{cr}	critical thickness showing transition from a global to only a local reinforcement effect;
$\Delta R/R_0$	relative change of resistivity;
ϵ	strain;
ϵ_{ave}	average strain experienced by specimen.

Subscripts

ext + SG	values determined with clip on extensometer, when specimen is simultaneously bonded to strain gauge;
gauge	gauge, i.e., measuring grid, properties;
loop	end-loops of strain gauge (Fig. 1);
PI	polyimide (carrier film) properties;
ref	reference values obtained by an extensometer for specimens with or without attached strain gauge;

sg used to indicate strain gauge measurements and properties of homogenized strain gauge;
spec properties of unreinforced test specimen (also relates to input values in simulation model).

Introduction

Strain gauges are commonly used strain measurement devices constructed from thin metallic grid, which is enclosed between polymer films (see Fig. 1). The working principle of the strain gauge incorporates the change of electrical resistance in the metal part linearly with its deformation [1]. Correlation between these two variables is expressed as the gauge factor [2], its determination is in more detail discussed later in subsection "Correction coefficient determination". During experimental testing the change of electrical resistance in the strain gauge is measured and converted into the strain values using the gauge factor.

This study is initiated by experimental observations, during which different elastic modulus values were obtained for identical polymer matrix based composite. The difference observed comparing the strain measurement from the strain gauge with the clip on extensometer. Deviations suspected to be caused by the stiffness mismatch between the strain gauge, which includes a thin metal grid, and the test sample, which is more compliant. Therefore the strain gauge induces strain reduction in the more compliant test sample [3] and promote strain distortions around the edges, where strains are transmitted from the test sample to the gauge [4, 5]. These phenomena are attributed to the effect known as the "reinforcement effect" [6]. As a result of the reinforcement effect, strain gauges measure lower strains compared with the strains experienced locally by the test sample in the absence of the strain gauge. This can lead to significant errors in determination of strain and elastic modulus. In spite of this, the standards often recommend the use of a strain gauge as an optional strain measurement device during mechanical testing of polymer and polymer matrix composite materials [7–9]. In addition to this, strain gauges are used to a great extent as strain identification sensors in composite structures.

One of the earliest studies regarding the strain gauge reinforcement effect are given by Stehlin [4]. Stehlin has modelled stress and strain distortions in the test sample, strain gauge and adhesive. This has been further applied by Beatty's and Chewning's [5] to conduct numerical analysis of strain gauge geometrical parameters such as thickness and length. These authors have provided an approximate expression to predict the local reinforcement effect, when strains are modified locally around an attached strain gauge and are found to be independent of specimen geometry. The expression indicates that reinforcement increases with stiffer and thicker strain gauges, whereas it decreases with longer strain gauges and stiffer specimens [5]. On the basis of theses studies, a more detailed discussion regarding correction of strain gauge measurements has been presented by Ajovalasit et al. [10–12]. First of all, the correction of the gauge factor obtained by conventional strain gauge calibration methods can be done [10] by correction coefficients derived from mathematical expressions. For that Ajovalasit et al. have provided improved mathematical expression based on deductions of Beatty and Cheawning [5]. Another approach involves strain gauge calibration on materials more compliant than the test samples [11]. The above mentioned studies were focussed on the local reinforcement effect estimation. Thus in the analytical and numerical models the specimen has been considered as a thick and semi-infinite plate having the same width as the strain gauge. The two dimensional problem has been considered for three dimensional calculations, in which the strain gauge and specimen have been defined as linear-elastic materials.

A similar approach has been used for the global reinforcement effect by Swan [13] and Little et al. [14]. Now the strain fields are not only localized by attachment of the stiff strain gauge material but also depends on the geometry of the test samples. Swan [13] deduced an approximate expression to predict the global reinforcement effect, which

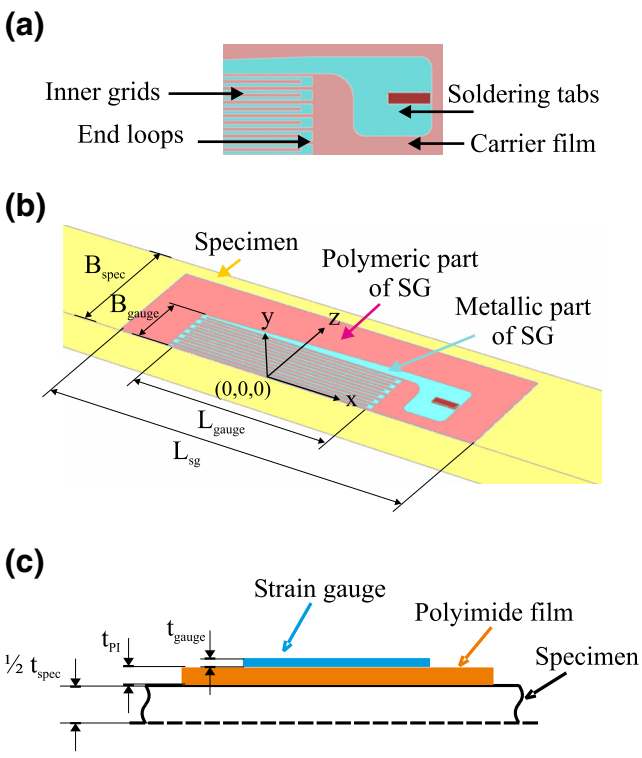

Fig. 1 Representation of strain gauge grid pattern (**a**), the 3D (**b**) and the 2D (**c**) simulation model

has been found to be proportional to the stiffness ratio of the strain gauge and the test sample as well as the thickness ratio. Moreover, Little et al. [14] observed that the reinforcement effect is affected not only by the specimen geometry, but also by the loading mode e.g. bending or tension.

Similar to strain gauges, fibre Bragg grating sensors have shown a reinforcement effect [15, 16]. Li et al. [16] has obtained a higher amount of reinforcement for fibre Bragg grating sensors, even though the elastic modulus of glass is much lower than that of the metal incorporated in strain gauge manufacturing. This was found to be due to the larger dimensions of glass fibres used for Bragg grating sensors.

In conclusion, the reinforcement effect was identified already in early studies of strain gauge implementation, where approximative mathematical expressions were presented in order to predict the strain gauge measurement errors coming from the local and global reinforcement effects. In the previous studies a simplified model of the strain gauge has been used homogenizing all parts of the strain gauge into one element. Therefore, the importance of the actual strain gauge pattern design has not been sufficiently discussed and error prediction has found to be limited. In addition, previous studies have been confined to elastic materials. Some research has been done to analyse gauge factor variations due to the plastic deformation of the metallic grid incorporated in the strain gauges [17–19]. Nevertheless, changes of the reinforcement effect due to plastic deformation both of the specimen and the strain gauge material has not previously been studied.

The purpose of the present study is to derive correction methods for the strain gauge experimental measurements, when a strain gauge is applied on specimens with elastic modulus in the range of 1-200 GPa and various geometrical dimensions. The finite element methods (FEM) are used to create detailed two (2D) and three (3D) dimensional models, in order to conduct a parametric study to assess the effect of specimen and strain gauge geometry with respect to the stiffness, both with the local and the global reinforcement effect. The 3D study of the strain gauge geometry is based on commercially available Y series strain gauges provided by the *Hottinger Baldwin Messtechnik GmbH* (HBM) company, but the results will not be limited to this. The study considers both elastic and plastic deformation in the strain gauge as well as in the test sample.

Methods

Simulation model

The commercial finite element code ABAQUS is used to create 2D and 3D numerical models of the experimental material set-up. This setup consists of a test sample with attached back-to-back strain gauges, which is subjected to tensile loading.

Parts

The test sample is modelled with a stiffness from 1 GPa to 200 GPa. The purpose is to cover the range of materials used for polymer matrix based composites and also to compare their response to metals. The thickness of the test sample is varied from 1 mm to 30 mm, so that both the global and the local reinforcement effect by the strain gauge is presented.

The detailed strain gauge pattern is included in the 3D model obtained from the micrographs (Fig. 1 (a), (b)) captured with a photo camera *Canon G9*. The width of the inner grids is set to 0.08 mm and the space between grids is 0.1 mm, which corresponds to the strain gauge type *LY11-10/350*. In the 2D plane stress simulation model, the strain gauge part is simplified as a uniform foil with half the thickness of gauge. This is due to merging the inner grids and the empty space between grids. Even though the 2D model is simplified, however similar to the 3D model, the distinction of the end loops, gauge and soldering tab area (Fig. 1 (a), (c)) is retained. For all strain gauge models the length of the end-loops is set to 3 % of the corresponding gauge length; a value, which corresponds quite well with the commercially available *HBM* strain gauges. The distinction of different strain gauge parts, what is done in this analysis, is contrary to previous studies [4, 5, 10–12], where a homogenised strain gauge model was preferred by merging all parts of the strain gauge including carrier film.

In order to exclude the effect of strain transition through carrier film and adhesive, a numerical calibration is conducted. The manufacturers provided gauge factor already includes these distortions, because it is obtained, while the commercial prototype of the strain gauge is glued on a steel surface [11]. Therefore numerical calibration involves determination of strain distortions applying different type of strain gauges, shown in Fig. 1, on a 200 GPa stiff and significantly thick material. The observed strain discrepancy of approximately 1 % is thus extracted from all the numerical results.

Material formulation

The metallic wire and the polymeric carrier film in the HBM Y series strain gauge is made of constantan and polyimide, respectively. The corresponding material properties are taken from Stockmann studies [20]. The polyimide carrier film is modelled as a linear-elastic material with E = 3.1 GPa and $\nu = 0.41$. The constantan is modelled as an elastic-plastic material with the elastic properties as E = 180 GPa

and $\nu = 0.3$, and the plastic deformation is described with Ludwik's equation:

$$\sigma = \sigma_y \left[1 + a(\phi)^n\right], \tag{1}$$

where the yield stress σ_y = 400 MPa, hardening parameters a = 4 and n = 0.45 and ϕ is the plastic deformation.

Constraints and elements

All material interfaces are modelled as perfectly bonded materials, thus are given as a tie constraint with no requirements of matching FE-meshes in the numerical procedure. A half model using 4 node isoparametric quadrilateral plane stress elements in the 2D representation, and a quarter of the model using 8 node isoparametric brick elements in the 3D representation of the test set-up is modelled using symmetric boundary conditions. The prescribed displacement boundary condition is used to mimic the tensile deformation.

Experimental testing

Validation of the simulation is done by performing tensile tests of a neat polymer and polymer matrix based glass fibre reinforced composites using a range of stiffness as E ∈ [1; 37] GPa and thickness as t_{spec} ∈ [1.5, 20] mm). The corresponding experiments are performed on a universal testing machine *Instron 88R1362* with a 5 kN (*SN: UK 802*) or a 100 kN (*SN: UK 1028*) load cell. Specimens with and without strain gauges *LY11-10/350* are tested using reference measurement methods with a laser extensometer (*'Fiedler Optoelektronik GmbH', PS-E50-0160-AH*) and a clip on extensometer (*Instron 2620-601, ± 5/50 mm*). Therefore two reference strain values of the test sample are presented. The first set of strain values is gained from the clip on extensometers mounting them on the samples with attached back-to-back strain gauges. The second set of strain values is measured by the laser extensometer, which is applied on the unreinforced test sample (the strain gauges are not attached to the test sample).

Correction coefficient determination

A correction coefficient, *C*, see equqtion (5), is defined in order to evaluate the error of strain gauge measurements and to provide gauge factor adjustment values [10]. The gauge factor, *GF*, of the strain gauge is defined as the ratio between the electrical resistance change and the deformation in the gauge:

$$GF = \frac{\Delta R/R_0}{\epsilon_{gauge}}, \tag{2}$$

where $\Delta R/R_0$ is the relative change of resistivity and ϵ_{gauge} is the strain in the gauge. Manufacturers provided strain gauges are calibrated on sufficiently large and stiff materials such as steel [11]. If the strain gauges are applied on compliant materials, new calibrations are needed, because the strain fields are changed due to the stiffness difference between the strain gauge and the specimen material. Additional calibration can be avoided by correcting manufactures' provided gauge factors as follows:

$$GF_{act} = \frac{GF_{cal}}{C}, \tag{3}$$

where GF_{act} is the actual gauge factor and GF_{cal} is the calibrated gauge factor provided by the strain gauge manufacturers. From equations (2) and (3) the strain gauge measurement error can be deduced as follows:

$$C = \frac{GF_{cal}}{GF_{act}} = \frac{\Delta R/R_0}{\epsilon_{sg}} \frac{\epsilon_{ave}}{\Delta R/R_0} = \frac{\epsilon_{ave}}{\epsilon_{sg}}, \tag{4}$$

where ϵ_{ave} and ϵ_{sg} are the strains experienced by the specimen and the strain gauge, respectively. The correction coefficient can also be expressed as the ratio of elastic modulus determined by the strain gauge (E_{sg}) and actual elastic modulus of material (E_{spec}):

$$C = \frac{\epsilon_{ave}}{\epsilon_{sg}} = \frac{\epsilon_{ave}\sigma}{\epsilon_{sg}\sigma} = \frac{E_{sg}}{E_{spec}}. \tag{5}$$

Results

The finite element model is first used to investigate the strain gauge caused strain disturbances in the test samples. This is followed by a parametric study to obtain the most significant strain gauge and test sample properties, which affect the correction coefficient of the gauge factor. The parametric study includes an analysis of the material stiffness, the strain gauge and the test sample geometrical properties, and the elastic-plastic material behaviour. Numerical results are compared to experimentally determined correction coefficients.

Strain gauge introduced strain disturbances

The accuracy of the strain gauge measurements depends on the amount of the reinforcement effect, which is caused by the stiffness discrepancy between the specimen and the strain gauge material. As shown in Fig. 2 as well as discussed by Little et al. [14] the reinforcement effect includes the strain reduction in the specimen and the strain distortions around the edges. The reinforcement effect can be split up into a local and a global part. The global part describes the phenomenon, where strains are modified through the

whole thickness with the attached strain gauge. The influence of the global reinforcement increases by reducing the specimen thickness and increasing the strain gauge geometrical dimensions, for more details see subsection "Correction coefficient influenced by specimen geometry" and "Correction coefficient influenced by strain gauge geometrical properties". By contrast, in the local part, strains are considered to change only close to the attached strain gauge and the effect of the test sample thickness can be eliminated.

In Fig. 2(a), the contour plots of the logarithmic axial strain component, ϵ_{11}, in a 3D model from the XY, XZ and XYZ planes are presented for the local reinforcement. The total region of distorted strains is approximately double the gauge length for a 1 GPa stiff specimen attached to the strain gauge type *LY11-10/350*. The contour plots reveal both a strain reduction below the gauge and a non-uniform strain distribution along the strain gauge width (z axis) and length (x axis) directions.

In the length direction, the strain distortions are mainly caused by the strain transition between materials with mismatching stiffness. These strain transition points are also illustrated in Fig. 2(b), where the normalized strain distribution along the specimen surface and inside the gauge is presented. Normalized strains are obtained dividing strains at the surface of the specimen by the average strain experienced over the whole specimen. Sharp peaks of the normalized strains are related to the edges where strains are transferred between the metal and carrier film, also the carrier film and the test sample. Peaks indicate very large and very low strain existence along the edges. Due to the strain distortions along the edges, inside the gauge the normalized strains tend to decrease close to the end-loops, which respectively affects the strain measurement accuracy of strain gauge devices.

In the width direction, in Fig. 2(a), which corresponds to the z axis, the strain field variations are smaller and depend more on the strain gauge pattern features. For example, it is observed that the strain drop in the gauge ends tends to be smaller when moving to the side edges of the test sample. Also the soldering tabs are found to lower the strain disturbances around the end-loops.

Correction coefficient influenced by the elastic modulus of specimen

Figure 3 shows the correction coefficient obtained by the 2D and the 3D simulation models for the test samples with different elastic moduli attached to the strain gauge

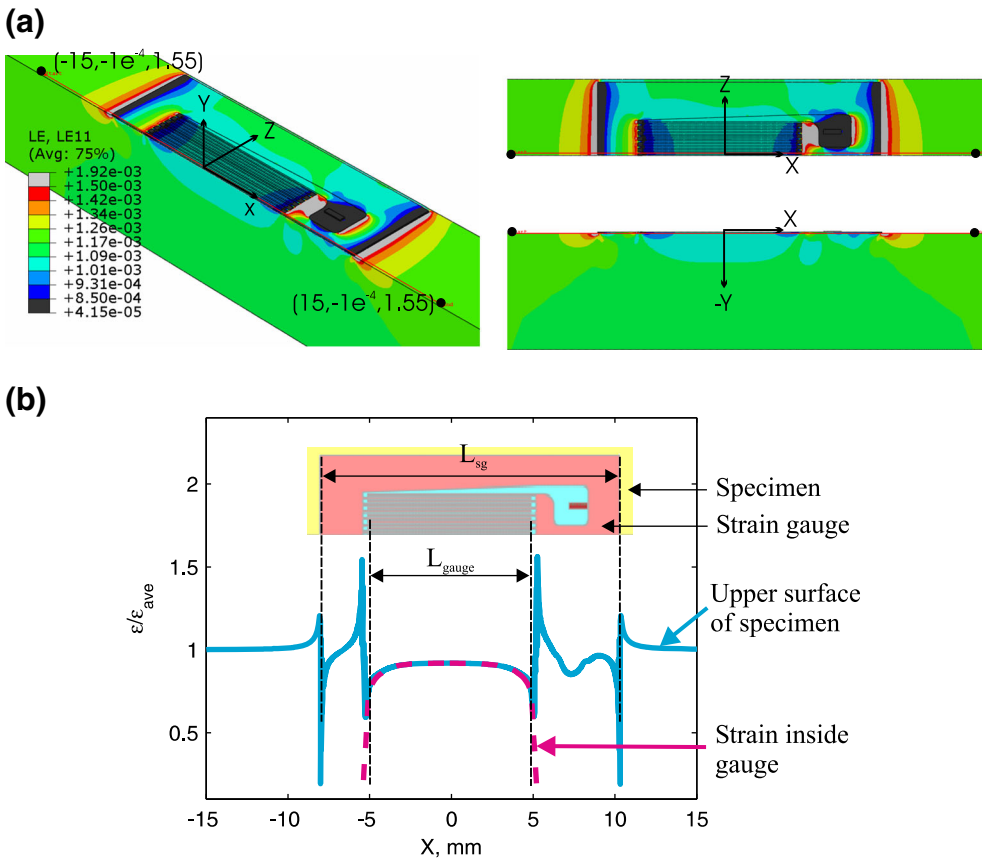

Fig. 2 Strain fields in the 3D model at ϵ_{ave} = 0.35 % (**a**) and normalized strain distribution along the specimen surface and inside the gauge obtained by the 3D model at ϵ_{ave} = 0.012 %. Strain path for specimen is between points (-15, -10^{-3}, 1.55) and (15, -10^{-3}, 1.55), and for the gauge including the end-loops between (-5.3, 4.8 x 10^{-2}, 1.55) and (5.3, 4.8 x 10^{-2}, 1.55) (**b**)

LY11-10/350. The 3D model predicts that the correction coefficient can be as high as 1.3 for the 1 GPa specimen, i.e., the strain gauge measurement error is 30 %. This is reduced by increasing the specimen stiffness, hence a 10 GPa stiff specimen has a correction coefficient around 1.04, i.e., a 4 % measurement error. A further increase of the test sample stiffness reduces the correction coefficient down to 1 %, therefore no error is expected for the test sample with E_{spec} = 200 GPa.

Along with the numerical results, in Fig. 3, experimental data are presented for an unreinforced polymer material test sample with t_{spec} = 4 mm and an attached strain gauge with L_{gauge} = 10 mm. Experimentally the elastic modulus is acquired using two different reference strain measurement methods, E_{ref}. The first experimental data point, noted as *Laser*, is obtained measuring strains with a laser extensometer for the test sample without attached strain gauges. Hence the elastic moduli for unreinforced test samples is noted as E_{spec}. The second data point, noted as *Extensometer*, is gained from the test samples with attached back-to-back strain gauges simultaneously with clip on extensometers, which are used to measure the actual strains in the test sample. Experimental results shown in Fig. 3 indicate that the correction coefficient (E_{spec} = 2.15 ± 0.01 GPa and E_{ext+sg} = 2.22 ± 0.01 GPa) is changed from 1.17 to 1.12, and thus is decreased by 5 %, implementing the second reference strain measurement method, E_{ext+sg}. Further in this paper, for most of the experimental results the correction coefficient is derived with the second method due to conveniences in experimental testing. This is underestimating the correction coefficient which is needed for actual test sample stiffness determination.

Furthermore, numerically the effect of the reference strain measurement method on the correction coefficient

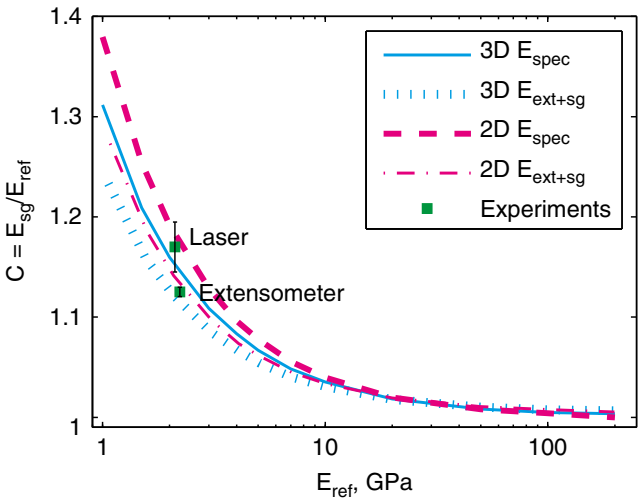

Fig. 3 Comparison between the 2D and the 3D models introducing different reference values (L_{gauge} = 10 mm, t_{spec} = 4 mm)

with the test samples stiffness is presented. The results obtained are shown in Fig. 3. Estimated values in 3D and 2D reveal that the difference between correction coefficients are 7.5 % and 10 %, respectively, for the specimen with an elastic modulus of 1 GPa. The deviation is gradually declining for stiffer test samples.

Correction coefficient influenced by strain gauge geometrical properties

Evaluation of the gauge thickness and length is presented for the strain gauges listed in Table 1. The correction coefficient rises linearly up to 3 % by increasing the gauge thickness from 3.8 to 5.0 μm, if t_{spec} = 30 mm and E_{spec} = 1 GPa. The larger correction coefficient changes are observed changing the gauge length from 1.5 mm to 10 mm. For example, in Fig. 4 the 2D model results show that the correction coefficient increases up to 1.52, i.e., the strain gauge measurement error is 52 %, if t_{spec} = 30 mm, E_{spec} = 1 GPa and L_{gauge} = 1.5 mm. Furthermore, the error is gradually reduced to 14 % for longer strain gauges with L_{gauge} = 10 mm.

In addition, the numerical results are compared with the analytical model derived for the local reinforcement effect by Ajovalasit et al. [10, 11] as follows:

$$C_{Ajovalasit} = \frac{\epsilon_{ave}}{\epsilon_{sg}} = 1 + \frac{E^*_{sg}}{E_{spec}}, \tag{6}$$

where E^*_{sg} is the reduced Young's modulus of the homogenized strain gauge, which characterizes the strain gauge sensitivity to the reinforcement effect and depends on the strain gauge stiffness, thickness and length [10]. The reduced Young's modulus for the strain gauges with L_{gauge} = 3 mm and L_{gauge} = 10 mm is given by Ajovalasit et al. [11] as 265 MPa and 175 MPa, respectively. Comparisons indicate deviations around 2.7 % for the strain gauges with L_{gauge} = 10 mm and increase up to 10 % reducing the gauge length to 3 mm.

Further study revealed that the correction coefficient dependency on the strain gauge length is related to the strain distortions inside the gauge. In Fig. 2(b) results show that the strain distribution in the gauge sections has a curved shape with higher strains in the middle section, which tend

Table 1 Geometrical dimensions of HBM strain gauges (*LY11-L_{gauge}/350*)[1]

L_{gauge} (mm)	B_{gauge} (mm)	t_{gauge} (μm)	L_{PI} (mm)	t_{PI} (μm)
1.5	1.2	5.0	5.7	45.0
3.0	1.5	5.0	8.5	45.0
6.0	2.9	5.0	13.0	45.0
10.0	5.0	5.0	18.5	45.0

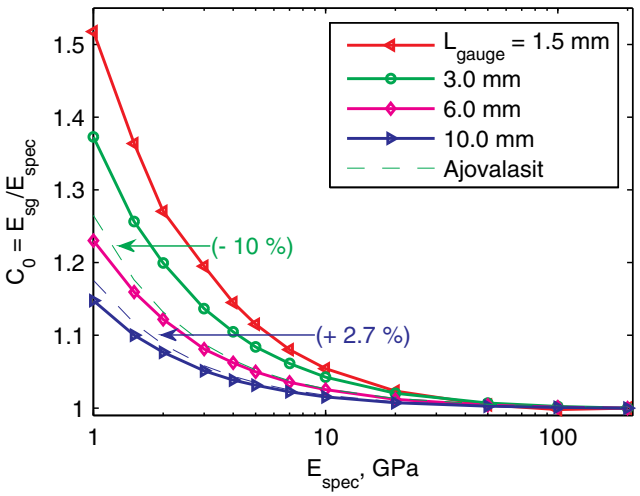

Fig. 4 The 2D simulation results presenting correction coefficient variations with strain gauge length (t_{spec} = 30 mm)

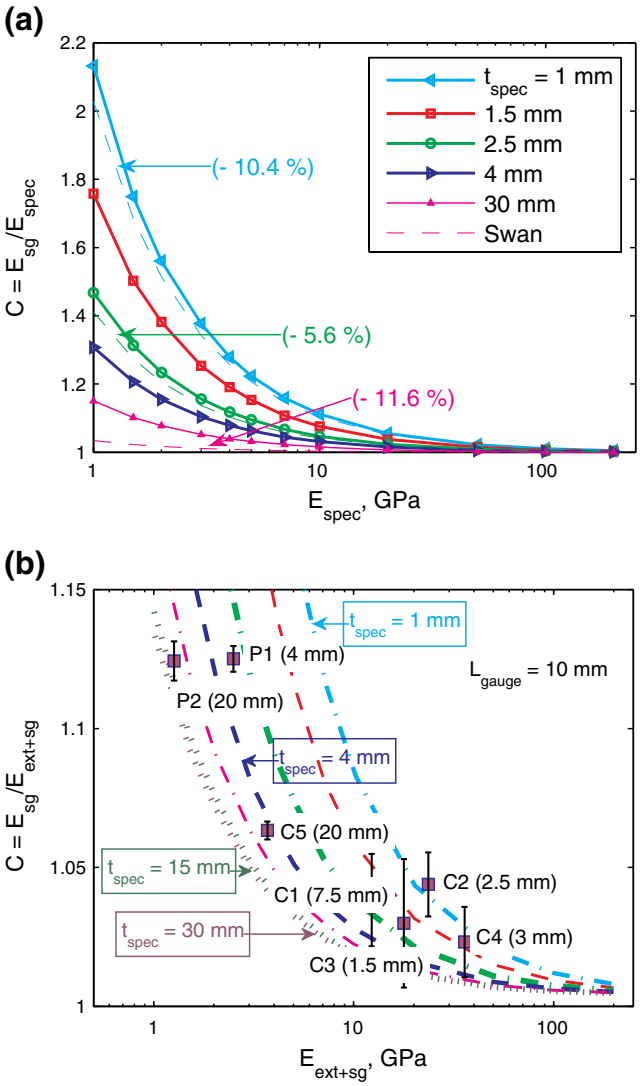

Fig. 5 The 2D model results presenting the correction coefficient variations with the specimen thickness and elastic modulus, if L_{gauge} = 10 mm

to approach the actual strain values of the test sample, and lower strains at the ends of the gauge. Analysing the strain distortions in the test samples, which are attached to the strain gauges with different lengths, it is observed that for shorter strain gauges the strains close to the ends reduce an average strain of the gauge more significantly. The reason is that for the shorter strain gauges the middle part of the gauge, which is unaffected by the edges, is narrower than is observed for the longer strain gauges. Therefore increasing the length of the strain gauge, the section of the gauge, which is unaffected by the edge effects, increases and contribute to higher accuracy of strain gauge measurements.

Correction coefficient influenced by specimen geometry

In the following subsection, the reinforcement effect sensitivity to the specimen dimensions such as width [10] and thickness [14] is discussed.

In Fig. 5(a), the 2D model results present the correction coefficient variations with the elastic modulus and the thickness of test sample, which is attached to the strain gauges with a gauge length 10 mm. Data obtained reveal a high sensitivity of the correction coefficient to the test sample thickness. Results show that for a 30 mm thick sample the correction coefficient is around 1.15 and it increases up to 2.18, i.e., obtaining 118 % of the strain gauge measurement error, when the test sample thickness is reduced to 1 mm. From Fig. 5(a) it is seen that the effect of the test sample thickness is larger for more compliant test samples. However, the reinforcement can still be significantly large even for relatively stiff, but thin test samples. For instance, the correction coefficient is as high as 1.15, which corresponds to a 15 % measurement error, if the elastic modulus and thickness of the test sample is 10 GPa and 1 mm, respectively.

Additionally, in Fig. 5(b) a comparison between numerical and experimental results is given. The experimental data are shown for the test samples with different thicknesses and material stiffnesses, which are attached to the strain gauges with a gauge length 10 mm. The largest correction coefficient values are obtained for the neat polymer materials noted as *P1* and *P2*, which are also the most compliant materials used in this study. In addition, these experimental results demonstrate the influence of the test sample thickness, i.e., even though *P2* is softer than *P1* it has the same correction coefficient value due to the thicker test sample. Further the correction coefficient descend for multi-axial glass fibre and polymer

matrix composites, noted as *C1*, *C2*, *C3*, *C4* and *C5*, which are around ten times stiffer than the neat polymer material test samples. From Fig. 5(b) it is seen that the correlation between the experimental correction coefficient and the test sample material stiffness follows the same tendency as it is numerically predicted. Nevertheless, the effect of the test sample thickness is not captured for composite materials. The authors suggest this is due to the substantially inhomogeneous structure of composites.

Numerical results are also verified with the analytical model proposed by Swan [13]. This model is intended for the correction coefficient determination, if a global reinforcement effect is present, and it can be calculated as follows:

$$C_{Swan} = 1 + \frac{2E_{sg}t_{sg}}{E_{spec}t_{spec}}, \tag{7}$$

with E_{sg} and t_{sg} as the elastic modulus and the thickness of an homogenized strain gauge, respectively. The elastic modulus of an homogenized strain gauge is taken from Ajovalasit et al. study [11]. Results, presented in Fig. 5(a), show that the analytically determined correction coefficients deviate from the numerical results by 5 % to 12 % depending on the test sample thickness.

Furthermore, the study shows that the impact of the test sample thickness on the correction coefficient determination is limited. In Fig. 6, the 2D predictions indicate the presence of a transition point at certain critical thickness, t_{cr}, after which the correction coefficient tends to saturate and retain permanent value, C_0. The critical thickness is attributed to the transition between the local and the global reinforcement by the strain gauge. The difference between these two reinforcement effects are described in subsection "Strain gauge introduced strain disturbances". The critical thickness obtained is found to be dependent on the strain gauge length, i.e., implementing shorter strain gauges the critical thickness is reduced.

In addition, the effect of the specimen width is evaluated by a 3D model, where t_{spec} = 10 mm and E_{spec} = 1 GPa. Increasing the specimen width from 10 mm to 20 mm the correction coefficient is reduced from 1.141 to 1.127, thus it is 2.5 % lower. The simulation results obtained agree well with the similar study done by Ajovalasit and Zuccarello [10], who also found that the width effect is negligible, when the width ratio of the specimen and strain gauge (B_{spec}/B_{sg}) exceeds 3.

Correction coefficient influenced by plastic deformation

The elastic-plastic material definition of the test sample is included to evaluate the correction coefficient changes at deformation levels exceeding the elastic region. In Fig. 7 the experimentally and in 2D correction coefficient obtained is presented for the specimen with dimensions 85 x 10 x 4 mm^3 and E = 2.1 GPa mounted on the strain gauge LY11-10/350. The correction coefficient is determined from the ratio of the strain measured by the extensometer and strain gauge according to equation (4).

The experimental results, shown in Fig. 7, indicate non-uniform correction coefficient values in the strain region of 0.05 % - 0.25 %, which is used for elastic modulus determination of polymers accordingly to the standard ISO 527-1 [7]. The observed non-uniformity of the experimentally determined correction coefficient is not known. Comparing averaged experimental correction coefficient values with numerical results the difference is below 5 %, which is considered as small.

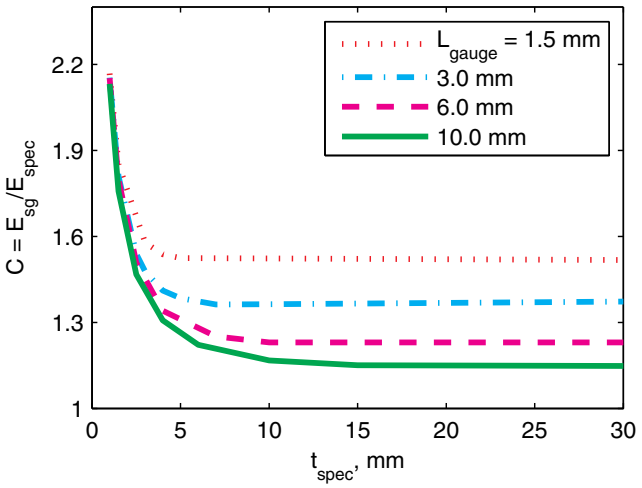

Fig. 6 The 2D model results presenting the effect of the specimen thickness on the correction coefficient applying different length strain gauges, if E_{spec} = 1 GPa

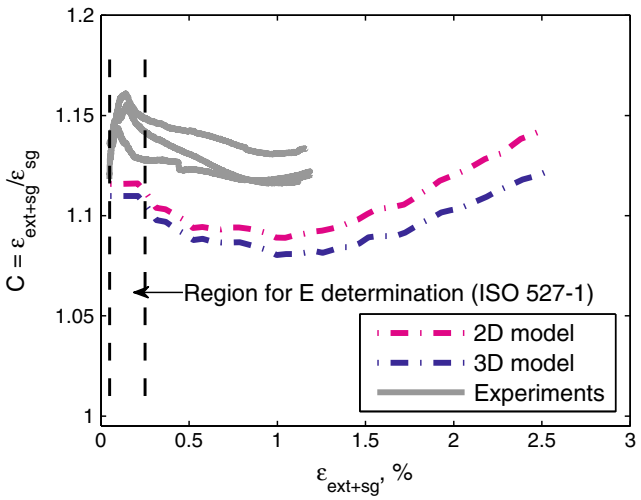

Fig. 7 Correction coefficient changes with plastic deformation (t_{spec} = 4 mm; L_{gauge} = 10 mm and E_{spec} = 2.3 GPa)

Beyond this deformation region the correction coefficient descends both for experimental and 2D results. In the 2D model, the correction coefficient starts to decrease at a strain of 0.24 %, whereas for some of the experimental results it is observed with even smaller values. The change of the correction coefficient is attributed to initiation of plastic deformation in constantan, which is the main component of the metallic parts in the strain gauge [2]. Continuing to deform the test sample above 1 % strain, the correction coefficient values again begin to rise. The ascending part is explained with more pronounced stiffness reduction by the test sample material during plastic deformation than it is in constantan.

Discussion on correction coefficient determination

Results revealed that the strain gauge measurement precision significantly alters with specimen stiffness and is considerably influenced by test sample and strain gauge geometry. The specimen thickness and the gauge length are found to be the most crucial geometrical dimensions. Generalizing results, the largest strain gauge measurement errors are expected for short strain gauges bonded to thin and compliant specimens.

In subsection "Correction coefficient influenced by specimen geometry", it is shown that the correction coefficient gradually decreases for thicker specimens, however the effect of thickness is limited. The numerical results predict that an increase of test sample thickness improves the strain gauge measurement precision only up to some critical value, i.e., t_{cr} - critical thickness. Further the enlargement of thickness has no impact on strain gauge measurements, and it is explained with a transition from a global to only local reinforcement effect. The critical thickness is dependent on strain gauge length and independent of specimen stiffness. Hence for each type of strain gauge the optimal test sample thickness can be determined to minimize the gauge measurement errors. In addition, if the optimal thickness is known then the effect of test sample thinning can be sufficiently well predicted by mathematical model provided by Swan [13]. The drawback of this model is that it does not provide any information about the transition between local and global reinforcement, and the optimal geometry of a specimen.

Furthermore, when the strain gauge is bonded on the test samples with a thickness above the critical one, the global reinforcement, i.e., strain distortions through the whole thickness, can be neglected. Therefore for thick test samples the reinforcement by the strain gauge is localized and the effect of the specimen geometry can be excluded. In the local reinforcement the strain gauge measurement accuracy depends mainly on the strain gauge geometry and the test sample stiffness. In subsection "Correction coefficient influenced by specimen geometry", the 2D results demonstrate the importance of strain gauge geometry. The strain gauge length is found as a dominating parameter affecting the measurement accuracy of commercially available strain gauges used in this study. The correction coefficient needed to adjust the strain gauge measurements is larger implementing shorter strain gauges, even though longer strain gauges contributed to a larger volume of total strain field disturbances. This phenomenon is explained with uneven strain distribution in the gauge, which is caused by the strain transition between materials with mismatching stiffness. For more details see subsection" Strain gauge introduced strain disturbances" and "Correction coefficient influenced by strain gauge geometrical properties".

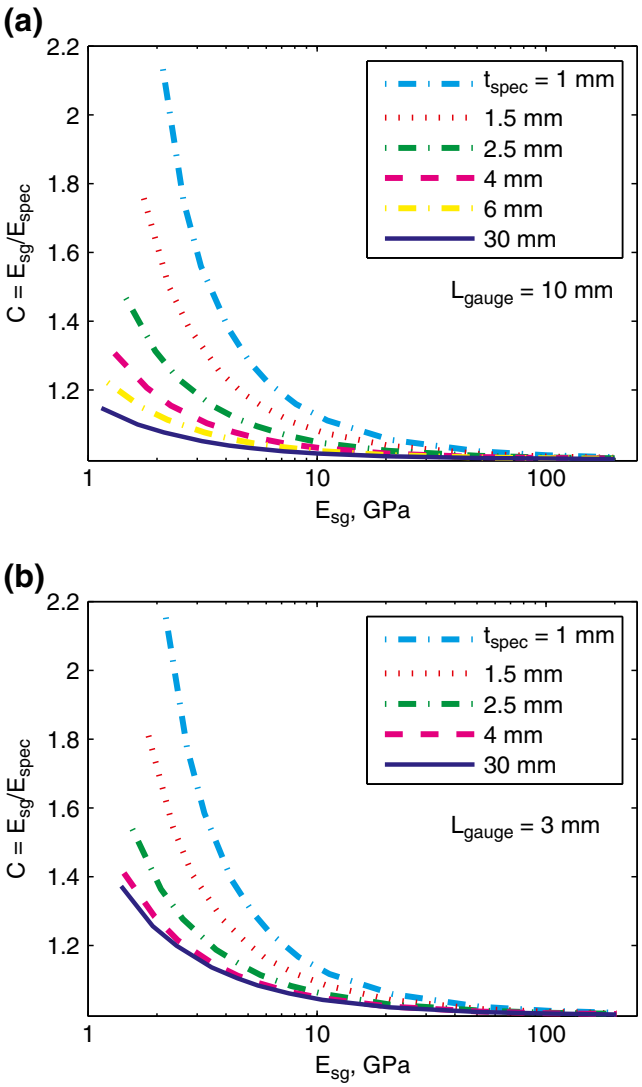

Fig. 8 Curves for strain gauge measurement correction, when L_{gauge} = 10 mm (**a**) and 3 mm (**b**)

In subsection“ Correction coefficient influenced by plastic deformation”, it is shown that plastically deforming the test sample the correction coefficient tends to decrease due to the plastic deformation of constantan. Nevertheless, it is expected that the resultant correction coefficient depends on the competition between plastic deformation of specimen and constantan. More pronounced stiffness reduction by the test sample will lead to an increase of the correction coefficient, and it will descent with larger stiffness reduction by constantan.

Practical determination of correction coefficient

The results reveal that the strain gauge measurement precision significantly depends on the specimen thickness, strain gauge length and amount of total deformation. Experimentally obtained strain gauge measurements can be modified by the correction coefficient considering the effect of these critical parameters. Otherwise calibration of the strain gauge on the specific test sample has to be performed. This study is focused on the adjustment of experimental results using numerically obtained correction coefficients accounting for the dominating local or global reinforcement effect.

In Fig. 8 the correction coefficient variations with elastic modulus determined by the strain gauge are presented for different specimen thicknesses. Therefore, the actual specimen's elastic modulus can be extracted using experimentally obtained strain gauge measurements and applying equation (5). The correction coefficient values are presented for specimens with attached strain gauges of type *LY11-10/350* (Fig. 8(a)) and *LY11-3/350* (Fig. 8(b)).

Figure 9 summarizes the results shown in Fig. 6 for the strain gauges with different lengths mounted on a 1 GPa stiff test sample. From this, a bi-linear correlation between the correction coefficient and the aspect ratio of the gauge length and the specimen thickness can be observed. A bi-linear correlation indicates a transition between locally and globally dominating reinforcement. Therefore above the critical thickness, i.e., lower values of L_{gauge}/t_{spec}, the correction coefficient is constant and indicates the local reinforcement dominating region. Decreasing the specimen thickness, i.e., increasing the values of L_{gauge}/t_{spec}, the correction coefficient tends to increase linearly and this is attributed to the global reinforcement dominating region. Depending on the current reinforcement effect the correction coefficient can be expressed as follows:

$$C = \begin{cases} C_0 + AL_{gauge}\frac{t_{cr}-t_{spec}}{t_{cr}t_{spec}}, & t_{spec} < t_{cr} \\ C_0, & t_{spec} > t_{cr} \end{cases} \quad (8)$$

By fitting a linear relation between the correction coefficient and L_{gauge}/t_{spec} for thinner specimens, a parameter A is extracted. In Fig. 10, conversion of the parameter A and the *permanent correction coefficient* with the test sample elastic modulus is demonstrated. It is found that the parameter A and the *permanent correction coefficient* both depend on the gauge length and elastic modulus of the specimen - tending to reduce with stiffer specimens. The *critical thickness* is found to be independent of the elastic modulus of the specimen, thus the *critical thickness* is estimated to be 3.3, 4.4, 6.5 and 9.5 mm for strain gauges with gauge lengths 1.5, 3.0, 6.0 and 10.0 mm, respectively.

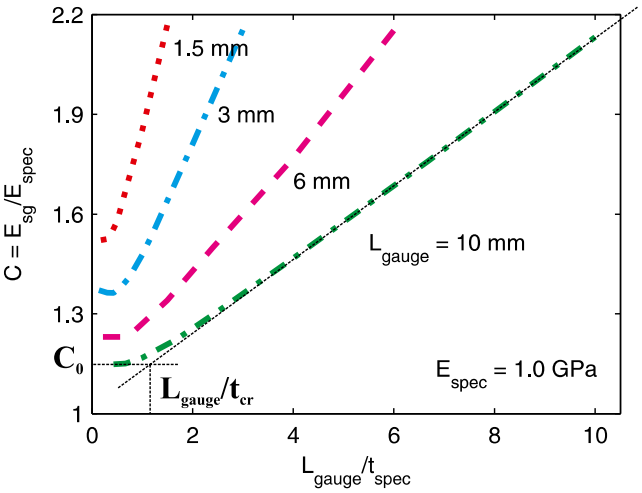

Fig. 9 The effect of specimen thickness and grid length on correction coefficient

Figure 11 presents the 2D model prediction of the correction coefficient variations for strains up to 5 % by including only the elastic-plastic material properties of the strain gauge metallic part. Simulation results are presented for the specimens with elastic modulus 1, 1.5, 3 and 10 GPa.

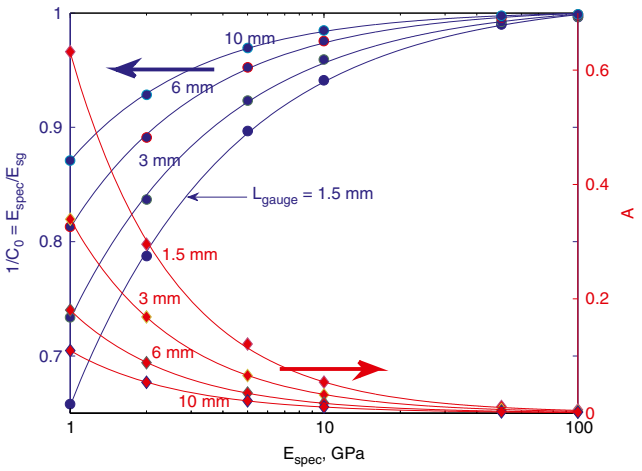

Fig. 10 Variations of parameters A and C_0 with material stiffness for strain gauges with different length (L_{gauge} = 1.5, 3.0, 6.0 and 10.0 mm)

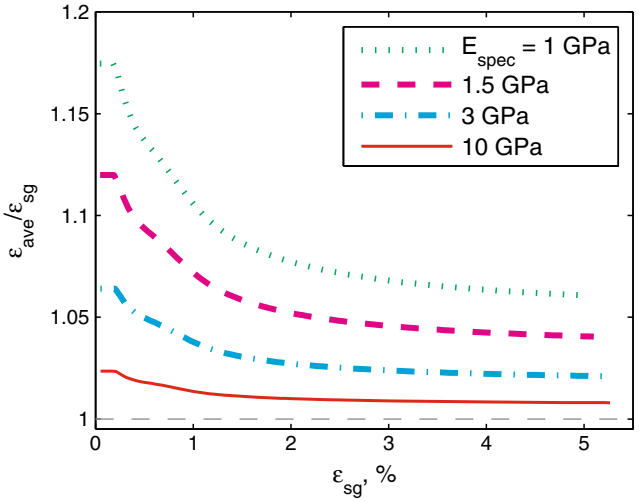

Fig. 11 The correction coefficient variation with large strains (t_{spec} = 30 mm; L_{gauge} = 10 mm)

The outcome demonstrates that the effect of the reinforcement will tend to decrease due to the plastic deformation of the constantan wire and softer materials will be more prone to the correction coefficient reduction. Nevertheless, the final *C* depends also on the specimen stiffness reduction as is shown in Fig. 7, where the correction coefficient increases due to the larger stiffness reduction by the specimen. Thus Fig. 11 allows one to determine the correction coefficient for a gauge factor, if the amount of specimen stiffness reduction with plastic deformation is known.

Conclusions

Results reveal that even for moderately stiff test materials sufficiently high correction coefficient values have to be used if short strain gauges are attached on thin test samples. Therefore the strain gauge length and the test sample thickness are found as the most significant geometrical dimensions. Depending on the correlation of these two parameters the dominating reinforcement effect by the strain gauge is divided into global and local ones. For each of the reinforcement effects different correction coefficient determination methods are applied. The transition between the global and only the local reinforcement effect is characterized with a *critical thickness*, above which only the local reinforcement effect exists. The *critical thickness* depends solely on the strain gauge length, thus can be used to optimize the test sample thickness.

In addition, it is observed that the correction coefficient tends to decrease due to plastic deformation of the strain gauge metallic part – constantan. Nevertheless, the resultant correction coefficient depends also on the test sample material deformation.

Acknowledgments This research was supported by the Danish Centre for Composite Structure and Materials for Wind Turbines (DCCSM), grant no. 09-067212, from the Danish Strategic Research Council (DSF).

References

1. HBM. Strain Gauge Catalog, www.hbm.com
2. Hoffmann K (1989) An Introduction to Measurements using Strain Gages
3. Perry CC (1984) The resistance strain gage revisited. Exp Mech 24(4):286–299
4. Stehlin P (1972) Strain distribution in and around strain gauges. The Journal of Strain Analysis for Engineering 7(3):228–235
5. Beatty MF, Chewning SW (1979) Numerical analysis of the reinforcement effect of a strain gage applied to a soft material. International Journal of Engineering Science 17(7):907–915
6. Watson RB (2008) Bonded electrical resistance strain gages. In: Sharpe WN (ed) Springer handbook of experimental solid mechanics, chapter 12. Springer, New York, pp 283–333
7. ISO 527-1: Plastics - Determination of tensile properties - Part 1: General principles, 1993
8. ISO 527-1: Plastics - Determination of tensile properties - Part 5: Test conditions for unidirectional fibre-reinforced plastic composites, 2009.
9. ASTM D5379/D5379M-12: Standard Test Method for Shear Properties of Composite Materials by the V-Notched Beam Method, 2012
10. Ajovalasit A, Zuccarello B (2005) Local reinforcement effect of a strain gauge installation on low modulus materials. The Journal of Strain Analysis for Engineering Design 40(7):643–653
11. Ajovalasit A, D'Acquisto L, Fragapane S, Zuccarello B (2007) Stiffness and Reinforcement Effect of Electrical Resistance Strain Gauges. Strain 43(4):299–305
12. Ajovalasit A (2011) Advances in Strain Gauge Measurement on Composite Materials. Strain 47(4):313–325
13. Swan JW (1973) Resistance strain gauges on thermoplastics. Strain 9(2):56–59
14. Little EG, Tocher D, O'Donnell P (1990) Strain gauge reinforcement of plastics. Strain 26(3):91–98
15. Luyckx G, Voet E, De Waele W, Degrieck J (2010) Multi-axial strain transfer from laminated CFRP composites to embedded Bragg sensor: I. Parametric study. Smart Materials and Structures 19(10):105017
16. Li W, Cheng C, Lo Y (2009) Investigation of strain transmission of surface-bonded FBGs used as strain sensors. Sensors and Actuators A: Physical 149(2):201–207
17. Ajovalasit A (2012) The Measurement of Large Strains Using Electrical Resistance Strain Gages. Experimental Techniques 36(3):77–82
18. Krempl E (1968) Evaluation of high-elongation foil strain gages for measuring cyclic plastic strains. Exp Mech 8(8):19N–26N
19. Rees DWA (1986) The sensitivity of Strain Gauges when Used in the Plastic Range. International Journal of Plasticity 2(3): 295–309
20. Stockmann M (2000) Micromechaniche Analyse der Wirkungsmechanismen elektrischer Dehnungsmessstreifen. PhD thesis, Technischen Universitat Chemnitz